Heterogeneous & Homogeneous & Bio- & Nano-

CHEMCATCHEM

CATALYSIS

# Accepted Article

**Title:** Peroxidase encapsulated in peroxidase mimics via in-situ assembly with enhanced catalytic performance

**Authors:** Xiaoling Wu, Jun Xiong, Shuli Liu, Bin Chen, Shan Liang, Wenyong Lou, and Min-hua Zong



**To be cited as:** *ChemCatChem* 10.1002/cctc.201902055

**Link to VoR:** http://dx.doi.org/10.1002/cctc.201902055

A Journal of

ChemPubSoc Europe

WILEY-VCH

www.chemcatchem.org

10.1002/cctc.201902055

WILEY-VCH

COMMUNICATION

# Peroxidase encapsulated in peroxidase mimics via *in-situ* assembly with enhanced catalytic performance

Xiaoling Wu*[a], Jun Xiong[a], Shuli Liu[a], Bin Chen[a], Shan Liang[a], Wenyong Lou*[a,b] and Minhua Zong[a]

**Abstract:** Enzymatic catalysis is of great importance due to its high catalytic activity and high selectivity. However, intrinsic fragile property of enzyme limits its application in a wide range, where inactive inorganic materials have proven promising in enhancing the stability of the enzyme in industry. Here, Prussian blue nanoparticles (PB) as peroxidase mimics were adopted for encapsulation of peroxidase, Cytochrome c (Cyt c). Prussian blue/Cytochrome c (PB@Cyt c) composite developed via *in-situ* assembly exhibited a 2.6-fold higher apparent enzymatic activity than the sum activity of equivalent Cyt c and PB due to synergistic effect. Mechanism investigation showed that interaction between irons ions from PB and carbonyl group and nitrogen from enzyme led to a favourable catalytic conformation of Cyt c. Moreover, PB shielded the encapsulated Cyt c against harsh conditions (e.g. high temperature and organic solvents). This new efficient hybrid catalyst would open opportunities for wide applications in biosensors and biocatalysis.

Bioactive molecules, with remarkable capability of manipulating plenty of substrates, tend to deactivate and lost their biological function when exposed to industrial conditions including high temperature and organic solvents.[1] The past decades have witnessed worldwide interest in the development of immobilized enzyme which intends to protect the enzyme from attack of extreme artificial environments.[2] In nature, one of the self-protection mechanism was biomineralization, where an inorganic shell formed around biomolecules during a biologically induced *in-situ* self-assembly process.[3] The inorganic shell endowed biomolecules with enhanced mechanical properties and protected them against harsh environments.[4] Learning from nature, researchers have developed a general method for encapsulating biomolecules into the inorganic nanostructure via *in-situ* assembly. Ge[5] and co-authors reported the first enzyme encapsulated in inorganic copper phosphate hybrid catalyst, where biomolecules formed a complex with copper ions and served as nucleation sites for further growth of copper phosphate shell. The resultant enzyme hybrid nanoflower exhibited remarkably enhanced thermal stability. The versatility of this process has driven the construction of bioactive molecules with protective inorganic shells including enzymes,[6] antibodies,[7] vaccine[8] and cells.[9] Moreover, nanostructured shells were not limited to metal phosphate crystals[10] and metal organic frameworks (MOFs).[11] The inactive carrier outside the enzymes has been regarded as one of the most effective strategies for protecting enzymes.

Another attempt to eliminate the environmental attack for enzymatic catalysis was via the *de-novo* design of inorganic nanostructured materials to mimic the complex structure and active site of the natural enzyme. Due to the relative inert property of the inorganic materials, inorganic enzyme mimics can be adopted in a wide operating range in harsh environments. To date, developed enzyme mimics can be categorized into three classes: carbon-,[12] metal-,[13] and metal-oxide-based[14] nanomaterials, according to their structure[15], which has found their potential applications in the biosensor development, diagnosis, cancer therapy, environmental protection and so on. For example, enzyme mimics serving as anticarcinogen has been rapidly developed in recent decades. In 2018, Qu and etc[16] fabricated homogeneous cerium oxide nanoparticles ($CeO_2$ NPs) with oxidase-like activity and ATP deprivation capacity, which exhibiting high efficiency in cancer therapy. Biomimetic $MnO_2$@PtCo nanoflowers[17] which can accelerate cascade intracellular chemical reaction to produce ROS were reported to induce cell apoptosis and thus significantly inhibit tumor growth. However, the catalytic activity of artificial enzymes still can not compete with natural enzymes.

In this study, the idea of integrating inorganic enzyme mimicry and natural enzyme was realized by utilizing Prussian blue nanoparticles (PB) with mimic peroxidase activity as protecting shell to encapsulate the native peroxidase Cytochrome c (Cyt c) (Scheme 1). Our research showed that Cyt c embedded into PB via *in-situ* assembly process exhibited “ultra-activity” due to the synergistic effect. The as-synthesized Prussian blue/Cytochrome c (PB@Cyt c) composite showed a 2.6-fold higher activity than the sum activity of equivalent Cyt c and PB. Moreover, owing to the shielding effect from PB, the encapsulated Cyt c showed enhanced stability when exposed to harsh reaction conditions (such as high temperature and organic solvents). The strategy proposed here is demonstrated to integrate enzyme with enzyme mimics to generate enhanced catalytic performance, thus, may provide a facile and versatile approach for fabrication of efficient hybrid biocatalysts in biosensors and biocatalysis.

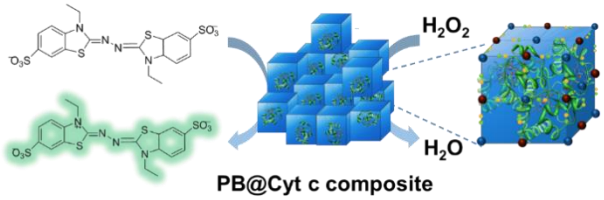


**Scheme 1.** Schematic showing preparation of PB@Cyt c composite via biomimetic mineralization.

[a] Dr. X. Wu, J. Xiong, S. Liu, B. Chen, S. Liang, Prof. W. Lou, Prof. M. Zong
Lab of Applied Biocatalysis
School of Food Science and Engineering
South China University of Technology
Guangzhou 510640 (P. R. China)
E-mail: wuxl18@scut.edu.cn
[b] Prof. W. Lou
Innovation Center of Bioactive Molecule Development and Application
South China Institute of Collaborative Innovation
Dongguan 221116 (P.R. China)
E-mail: wylou@scut.edu.cn

10.1002/cctc.201902055


# COMMUNICATION

The ultraviolet-visible (UV-Vis) spectrum (Figure 1a) of free Cyt c showed a peak at around 410 nm from the typical soret band of heme group of Cyt c, which can also be found in the PB@Cyt c composite, demonstrating the successful incorporation of Cyt c into the PB. Typical absorption at 700 nm from PB was observed in the freshly synthesized PB and showed a slightly shift to ~ 710 cm in the PB@Cyt c composite, indicating the possible interaction between Cyt c and PB. XRD patterns of PB@Cyt c composite showed diffraction peaks in line with PB (Figure 1b), implying the presence of Cyt c in the composite did not alter the cyanometalate structure of PB nanoparticles. The Cyt c loading amount in the PB@Cyt c composite was investigated by thermal gravity analysis (TGA) in the air (Figure 1c). As can be seen,in the range of 240 to 400°C, PB only exhibited 17 wt% of decomposition. While in the PB@Cyt c composite, an obvious decline of 47 wt% was observed. The apparently higher decomposition percentage can be attributed to the decomposition of Cyt c within this range, calculated to be 30 wt%. To further evaluate the encapsulation efficiency of this biomineralization, protein concentration in the supernatant immediately after the synthesis was measured by Coomassie brilliant blue assay. Almost no protein was detected in the supernatant, implying 100% encapsulation efficiency of this process, which was also consistent with the result of TGA. The dynamic light scattering (DLS) analysis showed that PB nanoparticles can be evenly dispersed in the aqueous solution (Figure 1d). Scanning electron microscopy (SEM) images of PB itself exhibited as nanocubes with a size of ~ 50 nm (Figure 1e),

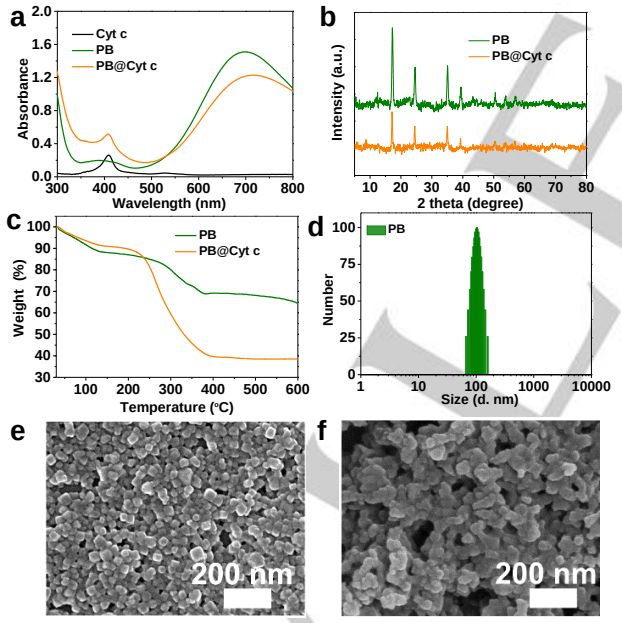


**Figure 1.** (a) UV-Vis spectra of Cyt c, PB and PB@Cyt c composite. (b) XRD patterns of PB and PB@Cyt c composite. (c) TGA analysis of PB and PB@Cyt c composite. (d) DLS measurement of PB in aqueous solution. (e-f) SEM images of PB (e) and PB@Cyt c composite (f).

which is consistent with the previous report.[18] After incorporation of Cyt c into the PB nanoparticles, a plate like structure was observed (Figure 1f), indicating that the introduction of protein interfered with the biomineralization. The enzymatic assay was performed by using hydrogen peroxide and ABTS as substrate. PB, as a peroxidase mimicry has been demonstrated [19] to show comparable activity with free Cyt c. When physically mixing free Cyt c with obtained PB (denoted as PB/Cyt c mixture), the activity of PB/Cyt c mixture was just sum up of activity of separate Cyt c and PB. While PB@Cyt c composite exhibited a 2.6-fold higher activity than PB/Cyt c mixture (Figure 2a). This enhanced activity was possibly attributed to the synergistic effects generated during the biomimetic mineralization.[20]

To demonstrate the above hypothesis, we investigated in-depth the interaction between Cyt c and PB by using Fourier transform infrared spectroscopy (FTIR), fluorescence spectroscopy and X-ray photospectroscopy (XPS) analysis together. As shown in Figure 2b, a strong absorption band around 2090 $cm^{-1}$ was ascribed to the characteristic stretching mode of C≡N from PB. The band at around 1650 $cm^{-1}$ which was ascribed to the amide I vibration can be found in the spectra of Cyt c. However, this peak showed a slight shift to higher wavenumber in the PB@Cyt c composite, confirming the successful incorporation of Cyt c during the biomineralization process. This shift also indicated that metal ions interact with the carbonyl groups, thus, regulating the activity of the encapsulated Cyt c. To further confirm the conformational change of PB@Cyt c after biomineralization, bands of amide I of enzyme in FTIR spectrum were analyzed. The contents of β-pleated sheet (1610-1640 $cm^{-1}$), random coil (1640-1650 $cm^{-1}$), α-helix (1650-1658 $cm^{-1}$) and β-turn (1660-1700 $cm^{-1}$) were calculated by using PeakFit 4.2 software.[21] As shown in Figure S1 and Table S1, random coil constituted 29.34% of the secondary structure in PB@Cyt c composite, which showed a 2.52% increase compared with that of free Cyt c. While β-pleated sheet of PB@Cyt c composite accounted for 14.42%, lower than that of free Cyt c. The increase of random coil and decrease of β-pleated sheet in PB@Cyt c may lead to a favorable secondary structure, which can partly explain hyperactivation of PB@Cyt c composite.[22] Fluorescence spectroscopy can reveal the tertiary structure change of protein. It is known that the active site of Cyt c lies in the heme group.[23] Moreover, four tyrosine residues and a tryptophan residue located near the heme group and thus affected the microenvironment of the active site.[24] The conformational change of these arranged amino acids around Cyt c can be reflected in the fluorescence spectra of Cyt c and affected the catalytic performance of the Cyt c.[25] As shown in Figure 2c, a 20 nm shift was observed in the fluorescence spectrum of PB@Cyt c composite with emission peak of 358 nm, demonstrating that the chemical interaction between free Cyt c and PB during the biomimetic mineralization process. The microenvironment change possibly resulted from the interaction of iron ions from PB with amide bond of Tyr67 residue of Cyt c, benefiting the consequent displacement of Met80 near the heme group and further exposure of heme group of Cyt c, which would promote catalysis,[26] and contribute to enhanced enzymatic activities.

To further reveal the local chemical environment of Fe ions, X-ray photoelectron spectroscopy (XPS) was carried out. The full spectra were shown in Figure 2d, showing the existence of Fe, C, N and H. The binding energy of Fe before and after the corporation of Cyt c was compared (Figure 2e). Peaks at 721.6 eV (Fe $2p_{1/2}$) and 713.1eV (Fe $2p_{1/2}$) were attributed to the FeNx

10.1002/cctc.201902055




unit. Peaks at 708.4 eV (Fe $2p_{3/2}$) were ascribed to $[Fe^{II}(CN)_6]$ group of PB. While in the high resolution XPS spectra of Fe in the PB@Cyt c composite, higher binding energy (708.6 eV) was observed, indicating the lower electron density of Fe. The N 1s high resolution spectra showed a positive shift from 397.6 eV in the PB to 400.2 eV in the PB@Cyt c composite (Figure 2f). The shift of binding energy of Fe and N together provided evidence that the self-assembly of Cyt c into PB was driven by the coordination between Fe ions and nitrogen from the amide bond of enzyme. Thus, results of XPS further corroborated that Cyt c interacted with PB via coordination during the biomineralization process thus altered the microenvironment of heme, which facilitated the displacement of Met80 near the heme group of Cyt c and benefited Cyt c-catalyzed peroxidase reaction.[26] Moreover, nitrogen from Cyt c may also interact with iron ions from PB and generate more catalytic active sites with structure similar to heme groups and catalyze the reaction. Thus, based on the above investigation, the enhanced apparent activity can be attributed to synergistic effect resulting from the change of microenvironment of Cyt c and the generated catalytic active sites between Cyt c and PB during the biomineralization process.

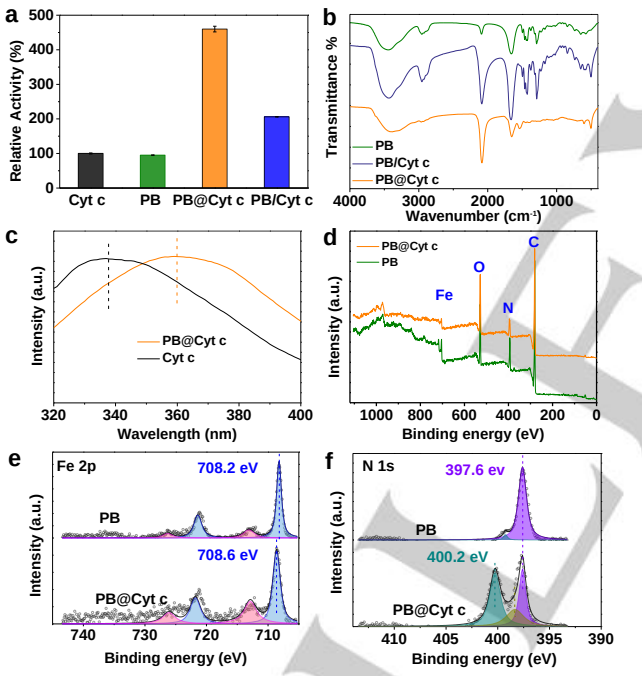


**Figure 2.** (a) Relative activity of PB, Cyt c, PB/Cyt c mixture and PB@Cyt c composite. (b) FTIR spectra of PB, PB/Cyt c mixture and PB@Cyt c composite. (c) Fluorescence spectra of Cyt c and PB@Cyt c composite. (d-f) XPS measurement of PB and PB@Cyt c composite. Full spectra (d), high resolution spectra of Fe (e) and N (f).

Kinetic parameters to evaluate the catalytic capability of PB, Cyt c, PB@Cyt c composite and PB/Cyt c mixture were obtained by fitting experimental data with Michaelis-Menten equation (Figure 3a, Figure S2 and Table S2). Free PB and Cyt c exhibited $K_m$ of 1.3 mM and 1.2 mM, respectively. After integrating Cyt c with PB via in-situ assembly, the obtained PB@Cyt c composite showed a slightly higher $K_m$ of 7.1 mM. As expected, PB@Cyt c composite showed $k_{cat}$ of 75.9 $s^{-1}$, which is 2.1-fold higher than the sum $k_{cat}$ of free PB and Cyt c, consistent with the enhanced enzymatic activity after biomineralization. Moreover, PB@Cyt c composite exhibited remarkably enhanced catalytic efficiency compared with PB/Cyt c mixture, with $k_{cat}/K_m$ of 10.7 $s^{-1}\cdot mM^{-1}$ for PB@Cyt c composite and 1.5 $s^{-1}\cdot mM^{-1}$ for PB/Cyt c mixture, respectively. These results further demonstrate that PB@Cyt c composite prepared via biomineralization exhibited improved catalytic capability.

Furthermore, the coating of PB around Cyt c provided shielding effect for encapsulated Cyt c, which endowed Cyt c enhanced stability when exposed to harsh conditions. The stability of enzyme under harsh conditions was vital for biochemical analysis. As can be seen in Figure 3b, when Cyt c was incubated in aqueous solutions under 80 °C for 3 h, it lost its original conformation, leading to exposure of heme group and increased activity of 3-fold was observed.[20] While the PB@Cyt c composite retained almost 100% of its activity, implying that the conformation of Cyt c encapsulated inside PB was retained. Moreover, enzyme molecules tend to go through a microenvironment change of active sites when exposed to organic solvents, which usually cause the loss of essential layer of water around and activity fluctuation thus, hindering its application in industry.[27] Here, free Cyt c and PB@Cyt c composite were incubated in water, dimethylsulfoxide (DMSO), acetonitrile (MeCN), and acetone (CP) at 30 °C for 30 min and samples were taken out for enzymatic assay. As shown in Figure 3c, free Cyt c exhibited 1.8-fold, 2-fold, 3-fold higher activity in DMSO, MeCN and CP than its reference in aqueous buffer, respectively. The hyperactivation of Cyt c after exposure to organic solvents would lead to poor reproducibility during industrial conditions with organic solvents. While almost no fluctuation of activity was observed in the sample of PB@Cyt c composite. The long-term storage stability of Cyt c after encapsulation was also measured (Figure 3d). Free Cyt c and PB@Cyt c composite retained almost 100% of activity even after incubated in aqueous buffer for 8 days under 37 °C, demonstrating its stability in aqueous solution. These results together suggested that PB shell around Cyt c during the biomimetic mineralization endowed the encapsulated Cyt c with enhanced stability against organic solvents and high temperature. Furthermore, the recycle performance of PB@Cyt c composite was investigated (Figure S3). PB@Cyt c composite retained 87.5% of its initial activity after 5 batches. After 10 cycles, PB@Cyt c composite loss 37.5% of activity, which was ascribed to the loss of nanoparticles and partly enzymatic activity during centrifugation process for next cycle. Thus, PB@Cyt c composite exhibited good reuse performance.

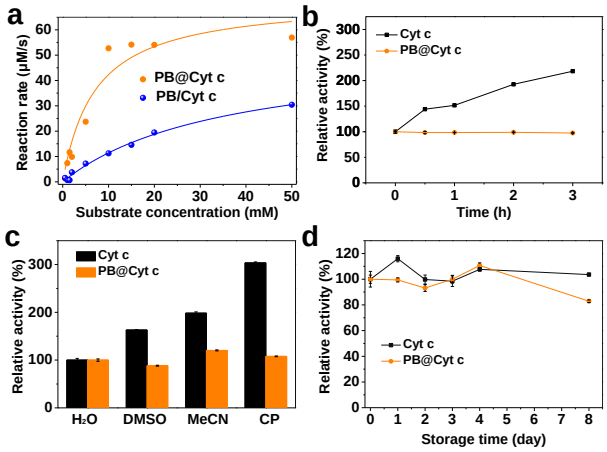


**Figure 3.** (a) Michaelis-Menten fitting of PB@Cyt c composite and PB/Cyt c mixture. (b-d) Operation stability at high temperature (80 ºC) in aqueous solution (b), under organic solvents (c) and storage stability (d) of Cyt c and PB@Cyt c composite.

In summary, peroxidase was in-situ encapsulated into peroxidase mimics via a biomimetic mineralization process. The as-synthesized PB@Cyt c composite exhibited a 2.6-fold higher apparent activity than that of simple mixture of PB and Cyt c. The enhanced apparent activity was attributed to the favorable conformational change of Cyt c during the biomimetic mineralization process. Moreover, PB provided protecting effect for the encapsulated Cyt c when it was exposed to inhospitable microenvironments including high temperature and organic solvents. This simple and facile approach of in-situ encapsulation enzyme molecules into inorganic enzyme mimics which can catalyze synergistically exhibited its potential in construction of hybrid catalyst systems for biocatalysis and biosensors.

## Experimental Section

Experimental details can be found in the Supporting Information.

## Acknowledgements

We acknowledge the financial support from the National Natural Science Foundation of China (21908070, 21676104, 21878105), the National Key Research and Development Program of China (2018YFC1603400, 2018YFC1602100), China Postdoctoral Science Foundation (BX20180102, 2019M652902) and the Fundamental Research Funds for the Central Universities (2019MS100, 2019PY15).

**Keywords:** Enzymes • Immobilization • *in-situ* assembly • synergistic effect

[1] a) F. H. Arnold, *Nature* **2001**, *409*, 253-257; b) U. T. Bornscheuer, G. W. Huisman, R. J. Kazlauskas, S. Lutz, J. C. Moore, K. Robins, *Nature* **2012**, *485*, 185-194; c) R. A. Sheldon, J. M. Woodley, *Chem. Rev.* **2017**, *118*, 801-838.

[2] a) X. Z. Lian, Y. Fang, E. Joseph, Q. Wang, J. L. Li, S. Banerjee, C. Lollar, X. Wang, H. C. Zhou, *Chem. Soc. Rev.* **2017**, *46*, 3386-3401; b) A. Küchler, M. Yoshimoto, S. Luginbühl, F. Mavelli, P. Walde, *Nat. Nanotechnol.* **2016**, *11*, 409-420; c) R. A. Sheldon, P. C. Pereira, *Chem. Soc. Rev.* **2017**, *46*, 2678-2691.

[3] a) F. Nudelman, N. A. J. M. Sommerdijk, *Angew. Chem. Int. Edit.* **2012**, *51*, 6582-6596; b) S. I. Stupp, P. V. Braun, *Science* **1997**, *277*, 1242-1248.

[4] a) A. Navrotsky, *Proc. Natl. Acad. Sci. U. S. A.* **2004**, *101*, 12096-12101; b) M. Mohammad, A. Razmjou, K. Liang, M. Asadnia, V. Chen, *ACS Appl. Mater. Inter.* **2019**, *11*, 1807-1820.

[5] J. Ge, J.D. Lei, R. N. Zare, *Nat. Nanotechnol.* **2012**, *7*, 428-432.

[6] a) F.J. Lyu, Y. F. Zhang, R. N. Zare, J. Ge, Z. Liu, *Nano Lett.* **2014**, *14*, 5761-5765; b) W. H. Chen, M. Vázquez-González, A. Zoabi, R. Abu-Reziq, I. Willner, *Nat. Catal.* **2018**, *1*, 689-695.

[7] Y. F. Feng, H. R. Wang, S. N. Zhang, Y. Zhao, J. Gao, Y. Y. Zheng, P. Zhao, Z. J. Zhang, M. J. Zaworotko, P. Cheng, S. Q. Ma, Y. Chen, *Adv. Mater.* **2019**, *31*, 1805148.

[8] M. A. Luzuriaga, R. P. Welch, M. Dharmarwardana, C. E. Benjamin, S. Li, A. Shahrivarkevishahi, S. Popal, L. H. Tuong, C. T. Creswell, J. J. Gassensmith, *ACS Appl. Mater. Inter.* **2019**, *11*, 9740-9746.

[9] K. Liang, J. J. Richardson, J. Cui, F. Caruso, C. J. Doonan, P. Falcaro, *Adv. Mater.* **2016**, *28*, 7910-7914.

[10] Z. X. Li, Y. F. Zhang, Y. C. Su, P. K. Ouyang, J. Ge, Z. Liu, *Chem. Commun.* **2014**, *50*, 12465-12468.

[11] X. L. Wu, J. Ge, C. Yang, M. Hou, Z. Liu, *Chem. Commun.* **2015**, *51*, 13408-13411.

[12] Z. W. Chen, Z. Z. Wang, J. S. Ren, X. G. Qu, *Acc. Chem. Res.* **2018**, *51*, 789-799.

[13] Y. H. Lin, J. S. Ren, X. G. Qu, *Acc. Chem. Res.* **2014**, *47*, 1097-1105.

[14] a) L. Z. Gao, J. Zhuang, L. Nie, J. B. Zhang, Y. Zhang, N. Gu, T. H. Wang, J. Feng, D. L. Yang, S. Perrett, X. Y. Yan, *Nat. Nanotechnol.* **2007**, *2*, 577-583; b) G. L. Li, P. Ma, Y. He, Y. F. Zhang, Y. N. Luo, C. Zhang, H. M. Fan, *Nano Lett.* **2018**, *18*, 5919-5926.

[15] Q. Sun, B. Aguila, S. Q. Ma, *Chem* **2018**, *4*, 2736-2738.

[16] F. F. Cao, Y. Zhang, Y. H. Sun, Z. Z. Wang, L. Zhang, Y. Y. Huang, C. Q. Liu, Z. Liu, J. S. Ren, X. G. Qu, *Chem. Mater.* **2018**, *30*, 7831-7839.

[17] Z. Z. Wang, Y. Zhang, E. G. Ju, Z. Liu, F. F. Cao, Z. W. Chen, J. S. Ren, X. G. Qu, *Nat. Commun.* **2018**, *9*, 3334.

[18] M. Vázquez-González, R. M. Torrente-Rodríguez, A. Kozell, W. C. Liao, A. Cecconello, S. Campuzano, J. M. Pingarrón, I. Willner, *Nano Lett.* **2017**, *17*, 4958-4963.

[19] a) M. A. Komkova, E. E. Karyakina, A. A. Karyakin, *J. Am. Chem. Soc.* **2018**, *140*, 11302-11307; b) J. X. Chen, Q. Q. Wang, L. Huang, H. Zhang, K. Rong, H. Zhang, S. J. Dong, *Nano Res.* **2018**, *11*, 4905-4913.

[20] H. Xia, X. Zhong, Z. X. Li, Y. B. Jiang, *J. Colloid Interface Sci.* **2019**, *533*, 1-8.

[21] J. J. Kong, S.N. Yu, *Acta Biochim. Biophys. Sin.* **2007**, *39*, 549-559.

[22] J. Bhasarkar, A. J. Borah, P. Goswami, V. S. Moholkar, *Bioresour. Technol.* **2015**, *196*, 88-98.

[23] W. R. Fisher, H. Taniuchi, C. B. Anfinsen, *J. Biol. Chem.* **1973**, *248*, 3188-3195.

[24] H. Edelhoch, *Biochemistry* **1967**, *6*, 1948-1954.

[25] W. R. Fisher, H. Taniuchi, C. B. Anfinsen, *J. Biol. Chem.* **1973**, *248*, 3188-3195.

[26] a) X. L. Wu, C. Yang, J. Ge, *Bioresour. Bioproc.* **2017**, *4*, 24-32; b) V. Yin, G. S. Shaw, L. Konermann, *J. Am. Chem. Soc.* **2017**, *139*, 15701-15709.

[27] A. Zaks, A. M. Klibanov, *J. Biol. Chem.* **1988**, *263*, 8017-8021.

10.1002/cctc.201902055

WILEY-VCH



**Entry for the Table of Contents** (Please choose one layout)

Layout 2:

## COMMUNICATION

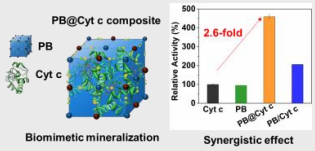


Peroxidase encapsulated in peroxidase mimics via in-situ assembly exhibited a 2.6-fold higher apparent catalytic activity and enhanced stability under harsh conditions.

*Xiaoling Wu*[a], Jun Xiong[a], Shuli Liu[a], Bin Chen[a], Shan Liang[a], Wenyong Lou*[a,b] and Minhua Zong[a]*

***Page No. – Page No.***

**Peroxidase encapsulated in peroxidase mimics via in-situ assembly with enhanced catalytic performance**